2002

The total molecular dipole moment for liquid water

Kusalik, Peter G.; Gubskaya, Anna V.

American Institute of Physics

Gubskaya, Anna V. and Kusalik, Peter G. (2002). "The total molecular dipole moment for liquid water". Journal of Chemical Physics, Vol. 117(11): 5290-5302.
http://hdl.handle.net/1880/44769
journal article

The total molecular dipole moment for liquid water

Anna V. Gubskaya and Peter G. Kusalik[a)]
Department of Chemistry, Dalhousie University, Halifax, Nova Scotia, B3H 4J3, Canada

(Received 26 April 2002; accepted 24 June 2002)

For the water molecule, the dipole is the first nonzero multipole moment; it represents the polarity of the molecule and has been widely used in describing solvation behavior. A rather wide range of theoretically determined values for the total molecular dipole moment of water in condensed phases has been reported in the literature. This paper describes a means by which the average total dipole moment for the water molecule in the liquid state can be linked to experimental refractive index data. Three components comprise the mean-field approach that is employed. A formal framework is developed that relates the temperature dependence of the effective molecular polarizability to the average local electric field experienced by a liquid water molecule over a chosen temperature range. A characterization of the distributions of local fields and field gradients is also necessary, and this has been determined from the computer simulations of liquid water samples at several different temperatures for two standard water potentials. The final component, the electric response properties of the water molecule (including nonlinear contributions up to fourth order), were determined from *ab initio* calculations for gas- and liquid-phase molecules, and are reported elsewhere [A. V. Gubskaya and P. G. Kusalik, Mol. Phys. **99**, 1107 (2001)]. By combining these three components, the temperature dependence of the average local electric field, and consequently the average total dipole moment, are extracted from data for the refractive index of liquid water. An almost 10% variation in the dipole moment with temperature is observed over the range 273 to 373 K. The value obtained for the molecular dipole moment at 300 K, 2.95 ± 0.2 D, is in excellent agreement with a recently reported result extracted from x-ray scattering data, as well as with some recent theoretical predictions. © *2002 American Institute of Physics.* [DOI: 10.1063/1.1501122]

I. INTRODUCTION

The dipole moment of a polar liquid, such as water, is a fundamental property of its molecules and is a basic ingredient for characterizing its local environment. While it may not be strictly possible to define a molecular dipole moment for water formally in condensed phase, it is nonetheless a very useful conceptual quantity. The molecular dipole moment of water has received a great deal of attention as it is known that the gas and liquid state values differ significantly and the apparently elevated values for liquid state molecules are important in our understanding the properties of liquid water. Yet, the dipole moment of individual water molecules in condensed phases cannot be measured directly, nor is there an unambiguous means of partitioning electron density among the individual molecules. Nevertheless, there have been many studies examining the dipole moment of the water molecule in various environments ranging from clusters to liquid water and ice[1–27] using a wide variety of theoretical models and computational techniques; some of these values have been summarized in Table I.

The total dipole moment of the water molecule in ice I_h was investigated by Coulson and Eisenberg[1] some 35 years ago using a simple induction model from which a value of 2.6 D was obtained. Surprisingly, this result has often been referred to in the literature as ''an experimental dipole moment for liquid water,'' whereas one would expect there to be a noticeable difference between the dipole moment of water molecules in ice and in liquid water. It is believed that the dipole moment of the molecule increases as a result of its interaction with neighboring water molecules; in this sense, water molecules in ice can be expected to be more polarized[2] and hence have a larger dipole moment. Recently, Batista *et al.*[3] re-evaluated the value of Coulson and Eisenberg[1] using the same induction model with more accurate data and including higher-order terms in the multipolar expansion. The dipole moment they determined was 3.1 D, i.e., significantly larger than the original result. A theoretical prediction based on dielectric properties and a Bernal–Fowler–Pauling ice-rules model of ice[4] gave a dipole moment of 3.0 D. Very similar values for ice were computed independently using density functional theory (DFT)[5,6] and MD simulations,[7] indicating that a magnitude of roughly 3.1 D is a realistic estimate for the molecular dipole moment.

The dipole moments calculated for liquid water typically range from 2.4 to 3.0 D (see Table I). The values obtained from *ab initio* calculations using molecular-based wave functions are surprisingly uniform (~2.7 D), whereas those found using plane wave approaches appear to depend strongly on the description (partitioning) of the molecular charge density.[2,5,8] The influence of local interactions within the liquid is ignored within the present mean-field approach. The *ab initio* studies of anions in ionic crystals by Fowler and co-workers[28–32] have identified the presence of large, short-range contributions to the induced multipoles in addition to the regular Coulombic contributions arising from

a)Electronic mail: kusalik@is.dal.ca

TABLE I. Selected estimates of the total dipole moment, m, of water in condensed phases.

Method	m (D) Ice	m (D) Water	References
Induction model	2.6		1
	3.1		3
BFP[a] model	3.0		4
Ab initio			
-DFT	2.3–3.0[b]		5, 6
-MP2		2.65	11
-MP2, MP4		2.7	10
-MP2		2.7	12
Ab initio MD		2.66	13
		2.43	2
		2.95	8
Classical potentials			
-nonpolarizable		2.1–2.4	18
-polarizable	3.1	2.73	7
		2.58, 2.65[c]	14
		2.51	15
		2.81 ± 0.25	16
		2.85	19
		2.88–3.03	17
Extracted from			
x-ray data		2.95 ± 0.6	9

[a]Bernal–Fowler–Pauling ice rules model.
[b]Depending on partitioning of charge density.
[c]Depending on the model chosen.

electric field and field gradient effects. The origin of these contributions has been attributed to the overlap of the cation and anion electron densities and results in a drop in the polarizability and hyperpolarizability of the anion.[28,29] As the local environment in liquid water differs considerably from that of an ionic crystal such as LiF, it is reasonable to expect that while these short-range contributions exist in water, they should be much less significant.[10] The work of Batista *et al.*[5] (see Fig. 2) perhaps suggests the presence of these effects in small water clusters and ice. Clearly, further careful investigation is needed to determine the importance of these effects in the condensed phases of water. We remark that such effects, which are neglected in the present mean-field treatment, would tend to decrease the expected value of the total dipole moment. The importance of inclusion of polarization effects has been shown previously by many authors (as reviewed in Ref. 7) and it is clear that most nonpolarizable potentials significantly underestimate the water dipole. The dipole moments produced by polarizable models span a moderate range (2.5–3.0 D). Encouragingly, the first experimental estimate of the water dipole has recently been given by Badyal *et al.*[9] based on x-ray scattering data for liquid water. Their reported result of 2.95 ± 0.6 D still spans a considerable range (including virtually all the values listed in Table I), although it perhaps suggests that the dipole moment for liquid water has been underestimated in most theoretical studies.

To the best of our knowledge, estimates of the average molecular dipole moment for liquid water and their temperature dependence have not been extracted previously from experimental data. Given the importance of this molecular property it would be very advantageous to be able to evaluate its temperature dependence from already existing, reliable, relatively easily determined experimental values. In this paper we will demonstrate how a detailed analysis of the refractive index for liquid water can be exploited for this purpose. The extraction procedure that will be employed will use a mean-field approach and will require detailed knowledge of the molecular response properties of water (as reported previously in Ref. 10) as well as characteristics of the average local environment experienced by a water molecule.

This article is organized as follows: The theoretical approach necessary to link experimental refractive index data, previously determined nonlinear optical polarizabilities (NOP),[10] and average values for the local electric field and field gradient is described in Sec. II. Numerical details and results from molecular dynamics (MD) simulations characterizing the distributions of local fields are given in Sec. III. In Sec. IV the results of the application of the present formalism, determination of the local electric fields, and evaluation of the total molecular dipole moment for liquid water are presented and discussed. Finally, our concluding remarks are given in Sec. V. We point out that unless explicitly indicated otherwise, values reported here will be given in atomic units, with the exception of temperature, which will always be in K.

II. GENERAL FORMALISM

The basis of the formal development that follows rests on a few key physical assumptions about the local microscopic environment of a liquid water molecule. The physical model that has been adopted is a mean-field approach[33–36] where a single water molecule is subject to a static electric field arising from neighboring molecules in the liquid, which has been described previously.[10] This approach then considers how the electric response properties of this molecule are influenced (relative to an isolated, gas-phase molecule) by this perturbing environment, characterized by the presence of an electric field and electric field gradient. The fundamental problem is that there exists no *a priori* criterion for selecting a partitioning scheme for the electron density (or the wave function) of the system. Three different estimates for the average dipole moment of liquid water molecules [2.43,[2] 2.66,[13] and 2.95 (Ref. 8)] have been reported for three different partitioning schemes. Batista *et al.*[5] have analyzed four algorithms for partitioning electronic charge density for small water clusters and for ice I_h. They concluded that these four different ways of the charge density partitioning lead to very different molecular dipole moments [e.g., in ice I_h the average dipole moment ranges from 2.3 to 3.1 D (Ref. 5)]. The present development assumes the water molecule is a well-defined entity in the liquid state and focuses exclusively on the electronic response of the molecule, where an electrostatic approach is assumed to be sufficient; such an approach has proven successful in our previous work.[10] Within this general framework we exploit the fact that the average local field experienced by a water molecule is nonzero only along the dipole vector, which we define to be its z axis. We then ultimately seek to parametrize the local elec-

trostatic environment in terms of this value and to connect it to the change in the measured electronic response properties of a water molecule in the liquid phase.

Our starting point in this development is the energy of the molecule. In the presence of an electric field and field gradient the energy of a polar–polarizable molecule can be represented as[37]

$$E = -\underline{\mu}_0 \cdot \underline{F} - 1/2\,\underline{\alpha} : \underline{F}\underline{F} - 1/6\,\underline{\beta} : \underline{F}\underline{F}\underline{F} - 1/24\,\underline{\gamma} : \underline{F}\underline{F}\underline{F}\underline{F} - 1/3\,\underline{\Theta}_0 : \nabla\underline{F} - 1/3\,\underline{A} : \underline{F}\nabla\underline{F} - 1/6\,\underline{B} : \underline{F}\underline{F}\nabla\underline{F} - \cdots, \quad (1)$$

where $\underline{\mu}_0$ is its permanent dipole moment, $\underline{\alpha}$ is the molecular polarizability, $\underline{\beta}$ is the first and $\underline{\gamma}$ the second hyperpolarizabilities, $\underline{\Theta}_0$ is the permanent molecular quadrupole moment, $\underline{A}$ and $\underline{B}$ are higher-order (dipole–quadrupole and dipole–dipole–quadrupole, respectively) polarizabilities. $\underline{F}$ and $\nabla\underline{F}$ are the electric field and electric field gradient, respectively. An expression for the total dipole moment, $\underline{m}$, of the molecule can be immediately obtained from Eq. (1) from the dependence of this energy on the electric field, explicitly

$$\underline{m} = -\frac{\partial E}{\partial \underline{F}}. \quad (2)$$

To proceed, we now consider the polarization response of a molecule to a small perturbing field, $\underline{f}$, while in the presence of a large field, $\underline{F}$, and field gradient, $\nabla\underline{F}$. Using the expression for the energy of this molecule [analogous to Eq. (1)] together with Eq. (2), we have that its total dipole moment is given by

$$\underline{m}(\underline{F}+\underline{f},\nabla\underline{F}) = \underline{\mu}_0 + \underline{\alpha}\cdot(\underline{F}+\underline{f}) + 1/2\,\underline{\beta}:(\underline{F}+\underline{f})(\underline{F}+\underline{f}) + 1/6\,\underline{\gamma}:(\underline{F}+\underline{f})(\underline{F}+\underline{f})(\underline{F}+\underline{f}) + 1/3\,\underline{A}:\nabla\underline{F} + 1/3\,\underline{B}:(\underline{F}+\underline{f})\nabla\underline{F} + \cdots. \quad (3)$$

For small $\underline{f}$, and taking advantage of the symmetry in the $\underline{\beta}$, $\underline{\gamma}$, $\underline{A}$, and $\underline{B}$ tensors, one obtains

$$\underline{m}(\underline{F}+\underline{f},\nabla\underline{F}) \approx \underline{m}(\underline{F},\nabla\underline{F}) + \underline{\alpha}^{\mathrm{eff}}(\underline{F},\nabla\underline{F})\cdot\underline{f}, \quad (4)$$

where

$$\underline{\alpha}^{\mathrm{eff}}(\underline{F},\nabla\underline{F}) = \underline{\alpha} + \underline{\beta}\cdot\underline{F} + 1/2\,\underline{\gamma}:\underline{F}\underline{F} + 1/3\,\underline{B}:\nabla\underline{F} + \cdots \quad (5)$$

is the leading order apparent molecular polarization response to the perturbing field, $\underline{f}$, in the presence of $\underline{F}$ and $\nabla\underline{F}$. In our physical model, where $\underline{F}$ and $\nabla\underline{F}$ represent liquid-phase conditions, $\underline{\alpha}^{\mathrm{eff}}(\underline{F},\nabla,\underline{F})$ will be the effective molecular polarizability as measured in the condensed phase.

Experimental values of the average molecular polarizability, $\overline{\alpha} = 1/3\ \mathrm{Tr}(\underline{\alpha})$, can be obtained by taking advantage of its relationship to the refractive index, n, determined at optical frequencies. The dependence of n on $\overline{\alpha}$ can be described using the Lorentz–Lorentz (LL) function.[38–40] For isotropic liquid phase conditions, the LL equation has the form[40,41]

$$\frac{n^2-1}{n^2+2} = \frac{4\pi\rho}{3}\overline{\alpha}(1+S), \quad (6)$$

where S is a small correction that depends on higher powers of the polarizability and the density, $\rho = N/V$. Determination of absolute values of $\overline{\alpha}$ from refractive index data for a liquid would require the evaluation of S. However, since S can be expected to be small (relative to 1),[41,42] changes in n due to changes in conditions of the system (e.g., temperature) will be dominated by the change in $\overline{\alpha}$ in Eq. (6); any change in S will be a higher-order effect and its influence should be small. By restricting our focus to changes in the molecular polarizability[43] we can ignore S and rewrite Eq. (6) in the conventional Clausius–Mossotti form for the refractive index

$$\frac{n^2-1}{n^2+2} = \frac{4}{3}\pi\rho\overline{\alpha}^{\mathrm{eff}}. \quad (7)$$

Clearly, accurate measurements of n and ρ for a liquid should provide estimates for the change in the average effective molecular polarizability, $\langle \underline{\alpha}^{\mathrm{eff}}(\underline{F}_l,\nabla\underline{F}_l)\rangle$, where $\underline{F}_l$ is the local electric field, i.e., the field experienced by any particular molecule within the liquid due to the surrounding molecular environment.

As we are focusing only on changes in $\underline{\alpha}^{\mathrm{eff}}$, Eq. (5) can be written as

$$\underline{\alpha}^{\mathrm{eff}}(\underline{F},\nabla\underline{F}) = \underline{\alpha} + \Delta\underline{\alpha}(\underline{F},\nabla\underline{F}), \quad (8)$$

where the components of the change in the effective molecular polarizability, $\Delta\underline{\alpha}(\underline{F},\nabla\underline{F})$, can be approximated in tensorial form as functions of hyper- and high-order polarizabilities [see the Appendix, Eqs. (A1)]. To make a connection to refractive index data, we must take the orientational average, and so we write that

$$\overline{\alpha}^{\mathrm{eff}} = 1/3\ \mathrm{Tr}(\underline{\alpha}^{\mathrm{eff}}) = \overline{\alpha}^{\mathrm{ref}} + \Delta\overline{\alpha}^{\mathrm{eff}}. \quad (9)$$

The second equality in Eq. (9) emphasizes that $\overline{\alpha}^{\mathrm{eff}}$ can be separated into fixed and variable contributions, where $\overline{\alpha}^{\mathrm{ref}}$ is the value of $\overline{\alpha}^{\mathrm{eff}}$ at some set of reference conditions. While the reference conditions could correspond to a gas phase molecule, we will see below that they can be conveniently chosen to be close to those of the liquid state. Taking into account the functional dependence of $\Delta\underline{\alpha}(\underline{F},\nabla\underline{F})$ upon the hyper- and high-order polarizabilities of the water molecule [see Eqs. (A1)], $\Delta\overline{\alpha}^{\mathrm{eff}}$ can be expressed as

$$\Delta\overline{\alpha}^{\mathrm{eff}}(\underline{F},\nabla\underline{F}) = 1/3[(\beta_{xxz}+\beta_{yyz}+\beta_{zzz})F_z + 1/2(\gamma_{xxzz}+\gamma_{yyzz}+\gamma_{zzzz})F_z^2 + 1/2(\gamma_{xxxx}+\gamma_{yyyx}+\gamma_{xxzz})F_x^2 + 1/2(\gamma_{xxyy}+\gamma_{yyyy}+\gamma_{zzyy})F_y^2 + 1/3(B_{xxxx}+B_{yyxx}+B_{zzxx})\nabla F_{xx} + 1/3(B_{xxyy}+B_{yyyy}+B_{zzyy})\nabla F_{yy} + 1/3(B_{xxzz}+B_{yyzz}+B_{zzzz})\nabla F_{zz}], \quad (10)$$

where the magnitudes for all components of the vector $\underline{F}$ are now values relative to the reference electric field and values of β, γ, and B are those for the reference state conditions. (Possible choices for reference state conditions, i.e., numerical values of the local field and field gradient for condensed phase calculations, have been discussed in Ref. 10.)

The average value of $\Delta\overline{\alpha}^{\text{eff}}$ can be determined by averaging over molecular configurations of the system. In the present model this becomes equivalent to integrating over the probability distribution functions for the local fields and field gradients. By symmetry $\langle F_x\rangle$ and $\langle F_y\rangle$ will be zero for the water molecule. In performing averages it is expedient to assume that the values of β, γ, and B are constants (i.e., are field-independent coefficients). We remark that this assumption becomes very good when the reference state condition is close to those of the systems of interest. We will see below that the appropriate field and field gradient distributions can be well approximated by Gaussian forms. Assuming that such forms are valid for real water expressions for $\langle F_z\rangle$, $\langle F_x^2\rangle$, $\langle F_y^2\rangle$, $\langle F_z^2\rangle$, $\langle \nabla F_{xx}\rangle$, $\langle \nabla F_{yy}\rangle$, and $\langle \nabla F_{zz}\rangle$ are easily evaluated. We have

$$\langle F_i\rangle = F_i^0, \tag{11}$$

and

$$\langle F_i^2\rangle = (\sigma_i^2 + (F_i^0)^2), \tag{12}$$

where the subscript i represents x, y, or z, σ_i is the width and F_i^0 is the center of the Gaussian [see Eq. (23)]. Clearly, only the first term in Eq. (12), which accounts for the difference between $\langle F_i^2\rangle$ and $\langle F_i\rangle^2$, will survive for $\langle F_x^2\rangle$ and $\langle F_y^2\rangle$.

To facilitate the development of our formalism, it is desirable for the final expression of $\Delta\overline{\alpha}^{\text{eff}}$ to be in terms of F_z^0 only. It is then clear from the discussion immediately above that it is necessary to assume that the average components of the field gradient and the fluctuations in the electric field can be expressed as simple functions of F_z^0. In particular, we choose to write that

$$\langle \nabla F_{ii}\rangle = d_{ii,0} + d_{ii,1}F_z^0, \tag{13}$$

$$\sigma_i^2 = e_{i,0} + e_{i,2}(F_z^0)^2, \tag{14}$$

where the subscript ii corresponds to diagonal components of the field gradient. Several points regarding these equations are noteworthy. From our analysis of simulation data for liquid water (discussed below) we have found that both Eqs. (13) and (14) give very good representations of results over the temperature range 263 to 373 K. Thus, the validity of the behaviors being assumed in Eqs. (13) and (14) is supported by these model results over a reasonable range of values. The constant terms, $e_{i,0}$ and $d_{ii,0}$, appearing in Eqs. (13) and (14), respectively, can be ignored in the further development as they will not contribute to $\Delta\overline{\alpha}^{\text{eff}}$. The values of the coefficients $e_{i,2}$ and $d_{ii,1}$ are unknown for liquid water, and hence we must rely on model calculations. In the present study we will assume that simple empirical potential models for water (specifically, TIP4P[44] and SPC/E[45]) provide a sufficiently accurate description of the local electrostatic environment to allow reasonable estimation of these values. The two models chosen are standard water potentials and are known to describe reasonably accurately the local structure in the liquid water near ambient conditions. Moreover, distributions of local fields and field gradients have unfortunately not been reported in recent *ab initio* studies[2,8,11–13] of liquid water.

Inserting Eqs. (11)–(14) into Eq. (10) and collecting terms yields the quadratic form

$$\Delta\overline{\alpha}^{\text{eff}} = a_1 F_z^0 + a_2 (F_z^0)^2, \tag{15}$$

where explicit expressions for a_1 and a_2 are given in the Appendix [see Eqs. (A2)]. These coefficients can be computed using the appropriate values of β, γ, and B from the *ab initio* calculations performed in our previous work,[10] together with the model-specific values $e_{i,2}$ and $d_{ii,1}$. It now remains to be shown how this relationship for $\Delta\overline{\alpha}^{\text{eff}}$, together with values for a_1 and a_2, can be utilized to determine the temperature dependence of the local electric field for liquid water.

In Eq. (15), the change in effective molecular polarizability, $\Delta\overline{\alpha}^{\text{eff}}$, is represented as a quadratic function of the local (average) electric field with coefficients a_1 and a_2. At the same time, we can express $\overline{\alpha}^{\text{eff}}$ and F_z^0 as simple functions of the temperature, T

$$\overline{\alpha}^{\text{eff}} = b_0 + b_1 T + b_2 T^2, \tag{16}$$

and

$$F_z^0 = c_0' + c_1' T. \tag{17}$$

We emphasize that the choice of these particular representations can be justified. Equation (16) reproduces the apparent quadratic temperature dependence of the effective molecular polarizability determined from the experimental data for the refractive index (see Fig. 3). In Sec. IV C we will discuss an alternate formulation that represents $\overline{\alpha}^{\text{eff}}$ as a quadratic function of $1/T$. The linear dependence in Eq. (17) is confirmed by the data for the average electric field obtained from MD simulations. (These results will be discussed in detail in Secs. III and IV B.)

We have already identified the constant term, b_0, appearing in Eq. (16) as $\overline{\alpha}^{\text{ref}}$, which corresponds to the value of $\overline{\alpha}^{\text{eff}}$ at some reference conditions. Since several unknown or undetermined factors contribute to this term, we will not be able to exploit it in our analysis. This consequence will have important implications, as we will discuss below. Nonetheless, defining $\underline{F}^{\text{ref}}$, the local electric field experienced by a water molecule under the reference conditions, it is possible to express Eq. (15) as

$$\Delta\overline{\alpha}^{\text{eff}} = a_1 \Delta F_z + a_2 \Delta F_z^2, \tag{18}$$

where

$$\Delta F_z = F_z^0 - F_z^{\text{ref}} = c_0 + c_1 T. \tag{19}$$

It is important to point out that the values of the a_1 and a_2 appearing in Eq. (18) must now be consistent with the reference conditions, $\underline{F}^{\text{ref}}$, and its possibly associated field gradient. Inserting Eq. (19) into Eq. (18), expanding, and then comparing terms with Eq. (16) yields

$$c_1 = -\sqrt{b_2/a_2}, \tag{20}$$

and

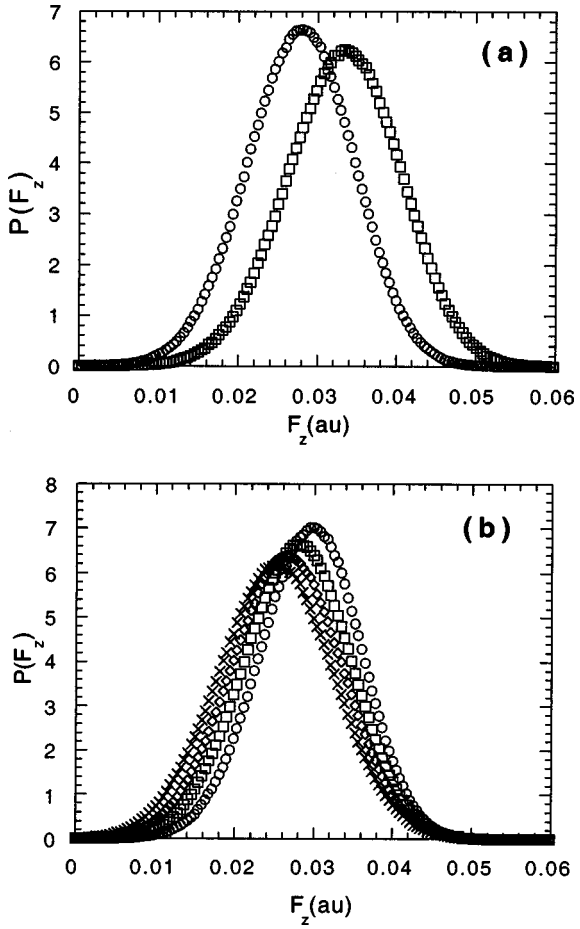

FIG. 1. (a) Probability distributions of the z component of the local electric field for SPC/E (squares) and TIP4P (circles) models at $T=298$ K. (b) Temperature dependence of the F_z probability distribution for TIP4P water. The open circles, squares, diamonds, and crosses represent results at 263, 298, 333, and 373 K, respectively.

$$c_0=(b_1/c_1-a_1)/2a_2, \tag{21}$$

where the coefficients b_1 and b_2 are obtained from the quadratic fit of the appropriate experimental data. The negative root appears in Eq. (20) because ΔF_z is expected to decrease with increasing temperature.

If one defines T^{ref} to be the temperature for which a water molecule experiences an average local electric field F_z^{ref} (i.e., $\Delta F_z=0$), then it is easily shown from Eqs. (19)–(21) that

$$T^{\mathrm{ref}}=(a_1c_1-b_1)/2b_2, \tag{22a}$$

$$c_0=c_1T^{\mathrm{ref}}, \tag{22b}$$

$$\Delta F_z=c_1(T-T^{\mathrm{ref}}). \tag{22c}$$

Thus, given the temperature dependence of the effective molecular polarizability obtained from measured refractive index data, as represented in the coefficients b_1 and b_2, together with characterization of the electric response properties of the water molecule contained in the coefficients a_1 and a_2, we can obtain the values for c_0 and c_1. Then, within the range of validity of Eq. (19) we can determine the average local field present in the liquid and hence the total dipole moment of the water molecule.

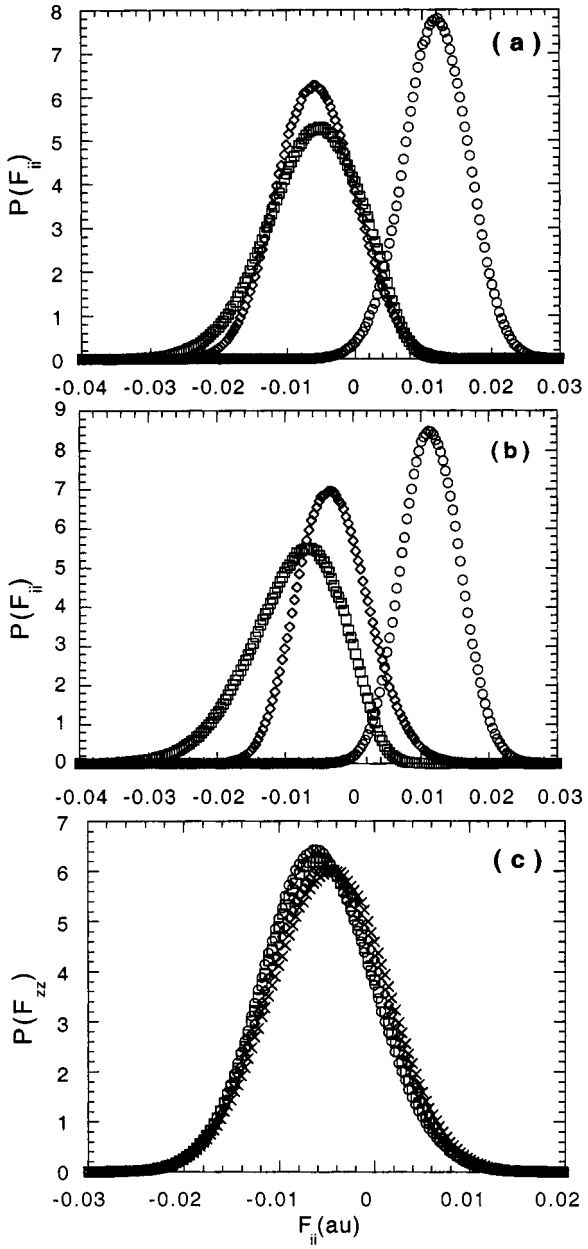

FIG. 2. Field gradient distributions for (a) SPC/E and (b) TIP4P water at $T=298$ K. The open circles, squares, and diamonds are results for $P(F_{xx})$, $P(F_{yy})$, and $P(F_{zz})$, respectively. (c) Temperature dependence of the F_{zz} probability distribution for SPC/E water. The symbols are defined as in Fig. 1(b).

III. ELECTRIC FIELD AND FIELD GRADIENT DISTRIBUTIONS

Molecular dynamics (MD) simulations have been performed with simple empirical water potential models in order to help characterize the local electric field and field gradient distributions present in liquid water. The SPC/E[45] and TIP4P[44] models were chosen because of their success in reproducing liquid state properties. This fact would suggest that they should be able to provide at least a semiquantitative picture of the local environment experienced by the water molecule; their ability to reproduce liquid water structure would indicate that they should provide a reasonable description of the fluctuations in the local field and the relationship

TABLE II. Electric field and field gradient components (in atomic units) of SPC/E and TIP4P water. Atomic unit conversion factors: 1 a.u.$=51.42$ V/Å; 1 a.u.$=5.142\times10^{-9}$ V/Å^2.

	SPC/E				TIP4P			
T(K)	$\langle F_z\rangle$	$\langle F_{xx}\rangle$	$\langle F_{yy}\rangle$	$\langle F_{zz}\rangle$	$\langle F_z\rangle$	$\langle F_{xx}\rangle$	$\langle F_{yy}\rangle$	$\langle F_{zz}\rangle$
263	0.0351	0.0131	−0.0072	−0.0059	0.0296	0.0128	−0.0100	−0.0029
298	0.0334	0.0119	−0.0062	−0.0057	0.0279	0.0115	−0.0086	−0.0029
333	0.0317	0.0109	−0.0057	−0.0052	0.0266	0.0105	−0.0078	−0.0028
373	0.0301	0.0100	−0.0052	−0.0048	0.0252	0.0097	−0.0071	−0.0026

between the field and field gradient. These MD simulations were carried out at constant experimental densities at temperatures of 263, 298, 333, and 373 K. A truncated octahedral simulation cell containing 256 particles was utilized. The Ewald summation technique[46] was used to calculate the Coulombic interactions and the electric fields. In the evaluation of the electric field gradients a spherical cutoff at $\sqrt{3}L/4$, the inscribed sphere radius, was employed. We remark that all fields and field gradients were measured at the center of the oxygen atom.

As already noted, only the electric field component along the molecular dipole vector (the z axis) will possess a nonzero average for reasons of symmetry. The distributions for the z component of the electric field for SPC/E and TIP4P water at a temperature of 298 K are shown in Fig. 1(a), where some difference in the widths and the positions of maxima is evident. TIP4P water has a slightly narrower distribution, which is also shifted to the lower values of the electric field, in comparison with the SPC/E result. Similar behavior is observed for all temperatures examined. The temperature dependence of the z-field distribution for TIP4P water [see Fig. 1(b)] reveals the sharpest distribution at $T=263$ K. The broadening of the distribution as the temperature is increased reflects the presence of larger fluctuations and structural disorder in the liquid at higher temperatures. We remark that, as expected, the electric field distributions in the x and y directions (not shown) have similar shapes but are centered about zero.

Distributions for all components of the electric field gradient were examined. Only the diagonal components xx, yy, and zz have nonzero average values, and field gradient distributions for these components are shown in Figs. 2(a) and 2(b), respectively, for SPC/E and TIP4P water at 298 K. Since the off-diagonal components of the field gradient do not contribute to the average field gradient experienced by a water molecule, only diagonal components will be considered further. The field gradient distributions are essentially symmetric, with both water models providing similar results. The most notable difference between the SPC/E and TIP4P results evident in Figs. 2(a) and 2(b) is the slight shift in the relative positions of the yy and zz distributions, where the latter model predicts field gradient values somewhat closer to those of an ideal tetrahedral structure.[10] The temperature dependence of the zz field gradient is given in Fig. 2(c) for the SPC/E model. We find only a slight broadening of the distribution and a slight shifting to a smaller average magnitude as the temperature increased.

As can be seen from Figs. 1 and 2, the field and field gradient distributions are well described by Gaussian functions

$$P(x)=Ae^{-k(x-x_0)^2}, \tag{23}$$

in which x_0 represents the average value, $k=1/2\sigma^2$, where σ is the width of the distribution and A is the normalizing factor. Consequently, all distribution curves were fit to Gaussian forms; average values of the nonvanishing components of the electric field and field gradient have been presented in Table II.

Electric field and electric field gradient distributions have been previously reported for liquid water by Nymand

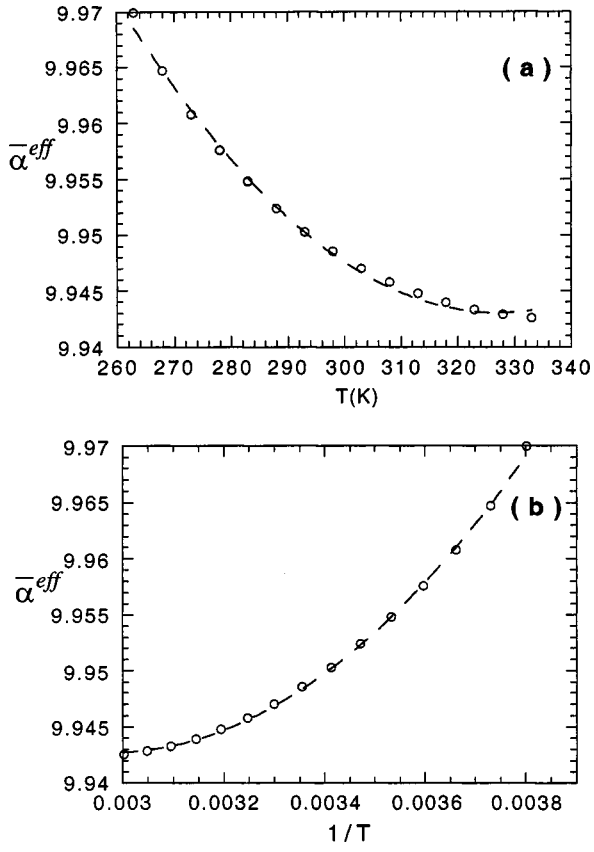

FIG. 3. Temperature dependence of the effective molecular polarizability determined from experimental refractive index data (Refs. 51–53) for liquid water. (a) The data plotted vs temperature where the dashed line represents a quadratic fit [see Eq. (16)] to these three sets of data; the coefficients of the fit are $b_0=10.607$, $b_1=-4.062\times10^{-3}$, and $b_2=6.209\times10^{-6}$. (b) The data plotted vs inverse temperature where the line represents the quadratic fit with the coefficients $b_0^*=10.283$, $b_1^*=-2.288\times10^2$, and $b_2^*=3.849\times10^4$.

TABLE III. Coefficients $e_{i,2}$ and $d_{ii,1}$ calculated from electric field and field gradient distributions.

Coeff.	$e_{x,2}$	$e_{y,2}$	$e_{z,2}$	$d_{xx,1}$	$d_{yy,1}$	$d_{zz,1}$
TIP4P	−0.028 79	−0.015 50	−0.051 54	0.718 67	−0.651 33	−0.068 37
SPC/E	−0.023 26	−0.026 87	−0.051 09	0.604 90	−0.397 27	−0.207 69

et al.[47,48] for the polarizable NEMO intermolecular potential.[49,50] They have reported the temperature dependence of the electric field at the oxygen as well as at the hydrogen atoms. Comparing the present data with those presented by Nymand *et al.*[48] for the electric field and field gradient at the oxygen atom, one can see that their numerical values for the electric field are significantly higher than those recorded in Table II. The NEMO potential also exhibits a stronger temperature dependence in the electric field.[47] Both observations are not surprising since both the SPC/E and TIP4P models represent effective nonpolarizable interaction potentials. The diagonal components of the field gradient in Table II generally exhibit the same decreasing trend (in magnitude) with increasing temperature. This is consistent with the results reported by Nymand *et al.*,[48] but again there are some differences in the magnitudes of the field gradient components. The behavior of the field gradient distributions appears to be more sensitive to the choice of molecular model for water and temperature (i.e., upon the details of the local structure) than those for the electric field. We remark that the probability distributions for the local electric field obtained here are in good agreement with results from the simulation study of Bursulaya *et al.*[14] employing *ab initio* potentials.

IV. RESULTS AND DISCUSSION

A. Application of general formalism

Within the general formalism proposed here, the dependence of $\Delta\overline{\alpha}^{\text{eff}}$ on the local electric field must be matched to the behavior inherent in the experimental data. It is the experimental temperature dependence of the effective molecular polarizability, $\overline{\alpha}^{\text{eff}}$, that is utilized. As was discussed in Sec. II, the molecular polarizability can be easily extracted from measurements of the refractive index by taking advantage of its functional relationship to the molar refractivity (Lorentz–Lorentz function). In the present study the effective molecular polarizability of H_2O has been calculated [using Eq. (7)] from a composite of three sets of experimental refractive index data[51–53] for liquid water at a wavelength of 589 nm (sodium D line), and over the temperature range from 263 to 333 K. The refractive index data for water by Tilton and Taylor[51] have recently been augmented by Saubade[52] and by Hall and Payne,[53] and these three sets were concluded to be among the most reliable, in accord with Schiebener *et al.*[40] A single set of values for the polarizability, $\overline{\alpha}^{\text{eff}}$, was obtained and its temperature dependence is shown in Fig. 3. Quadratic fits to this data and the corresponding coefficients are also included in Fig. 3. We note that we have also examined data given by the two general fits for the refractive index for water given by Schiebener *et al.*;[40] we have confirmed that our final results are virtually unchanged if the fit of Schiebener *et al.*[40] optimized for liquid water is used.

Before proceeding to the application of our formalism, some important points should be reviewed. First, two additional sets of coefficients (derivative from our MD simulations) are needed, $e_{i,2}$ and $d_{ii,1}$. The coefficients e_i accounting for the difference between $\langle F_i^2\rangle$ and $\langle F_i\rangle^2$ (i.e., the fluctuations in electric field about its average value) were determined with Eq. (14) from the dependence of the widths of our electric field distributions. The coefficients d_{ii} allow $\Delta\overline{\alpha}^{\text{eff}}$ to be expressed only in terms of the average electric field by replacing the dependence on the average field gradient, $\langle\nabla F_{ii}\rangle$, in Eq. (10) by the corresponding function of $\langle F_z\rangle$. Values of the coefficients $e_{i,2}$ and $d_{ii,1}$, as determined from our MD simulations for both TIP4P and SPC/E models, are given in Table III. We emphasize that the values of these two coefficients are the only elements of the present formalism that depend upon our classical simulation results, where $d_{ii,1}$ represents the linear correlation between the average field and field gradient and $e_{i,2}$ relates the magnitude of the fluctuations in the local field to the value of the average field.

In order to determine the sets of coefficients a_1 and a_2, values of NOP obtained from *ab initio* calculations [see Eqs. (A2) and Ref. 10] as well as the sets of coefficients given in Table III, are utilized. The coefficients a_1 and a_2 combine the NOP previously calculated using quantum chemical approaches[10] with the electric field (and field gradient) distribution properties obtained from MD simulations. We recall that to reproduce a local environment representative of the liquid state in our previous *ab initio* calculations (for NOP) three liquid-phase mean-field models were investigated.[10] In each case these models serve to define a particular set of reference conditions [i.e., $\underline{F}^{\text{ref}}$, Eq. (19)]. Model I assumes a

TABLE IV. Coefficients a_1 and a_2 for the local field dependence of $\Delta\overline{\alpha}^{\text{eff}}$ as determined from molecular response properties and characteristics of the field and field gradient distributions. The B values used are those determined with the POL basis set (see Ref. 10).

Distribution coefficients	Model 0b		Model I		Model II		Model III	
	a_1	a_2	a_1	a_2	a_1	a_2	a_1	a_2
TIP4P	−25.26	382.86	−1.18	613.41	−15.12	583.51	−15.71	573.81
SPC/E	−20.75	376.45	4.45	606.18	−5.41	570.77	−7.46	563.9

TABLE V. Coefficients c_0 and c_1 for the temperature dependence of the average local electric field as extracted from experimental refractive index data for liquid water.

Distribution coefficients	Model 0b		Model I		Model II		Model III	
	c_1	c_0	c_1	T^{ref}	c_1	T^{ref}	c_1	T^{ref}
TIP4P	−0.000 128	0.075	−0.000 101	337.2	−0.000 103	453.2	−0.000 104	459.4
SPC/E	−0.000 128	0.070	−0.000 101	291.3	−0.000 104	373.0	−0.000 105	390.8

strong electric field of 0.03 a.u. applied to the water molecule along its z axis. Model II is defined by a strong electric field (0.03 a.u.) and a highly symmetric field gradient ({0.008, −0.008, 0}). In model III, an electric field of 0.032 a.u. and a less symmetric field gradient of {0.01, −0.006, −0.0038} are present. We remark that the numerical values of field and field gradient for model III were chosen to mimic the characteristics of the MD simulations results reported in Sec. III. For all three liquid-phase models the nonlinear optical polarizabilities α, β, γ, and B were determined. The computational scheme described in our previous work[10] was also used to calculate these NOP for a gas-phase (isolated) molecule (which experiences neither fixed field nor field gradient). A more detailed discussion can be found in Ref. 10.

Table IV gives values for a_1 and a_2, obtained when results from the SPC/E and TIP4P simulations are coupled with values of NOP for gas phase (models 0) and for the three liquid-phase mean-field models of water. The coefficient a_1 contains contributions from both β and B dependent terms (approximately 50% coming from each when the $d_{ii,1}$ coefficients have been used), while a_2 depends only on γ. The coefficients c_0 and c_1 finally link the behavior found in the experimental data of the refractive index (effective polarizability) to the results for the field dependence of $\bar{\alpha}^{\text{eff}}$ (characterized by a_1 and a_2). These coefficients are calculated using Eqs. (20)–(22) together with values of b_1 and b_2 from Fig. 3(a); results for c_0 and c_1 are summarized in Table V.

B. The local electrical field

On the basis of the accurate values for the NOP of the water molecule determined in previous work,[10] MD simulations performed here, and experimental refractive index data, the average local electrostatic environment of a water molecule in the liquid phase can be predicted over a range of temperatures. It follows from Eq. (19) that

$$\langle F_z \rangle = F_z^{\text{ref}} + c_0 + c_1 T, \tag{24}$$

where F_z^{ref} is the reference value for the electric field (0, 0.03, or 0.032 a.u.), and c_0 and c_1 (see Table V) are given by Eqs. (20) and (21). We point out that in the discussion below we will focus on the numerical values of the average electric fields predicted by Eq. (24) when contributions due to fluctuations in the field have always been included (through the coefficients $e_{i,2}$). We have found that omission of these field fluctuation terms results in a 10%–14% reduction in the magnitudes of the local fields.

Within the present approach, the values of NOP for models I, II, and III coupled with parameters obtained from MD simulations for SPC/E and TIP4P water (henceforth models I_S and I_T, II_S and II_T, III_S and III_T, respectively) were used to extract estimates for average electric fields from 263 to 373 K. These results are shown in Fig. 4. It is particularly interesting to compare the predicted electric fields at temperatures of 298 and 263 K, where the latter corresponds to a structurally more ordered "supercooled" liquid. At $T = 263$ K, electric fields of 1.68, 2.13, 2.23 V/Å were obtained for models I_S, II_S, and III_S, respectively. The results for the models coupled with TIP4P data (I_T, II_T, and III_T) are approximately 15%–20% higher. At $T = 298$ K the electric fields have decreased slightly in magnitude, by about 8%, in all cases. In general, lower electric field values for models coupled with SPC/E distribution characteristics are observed in comparison with those based on TIP4P result over the entire temperature range.

The temperature dependence of the predicted electric fields for model I (i.e., taking into account only the perturbing effects of the local electric field) can be compared directly with those from models II and III (which include field gradient effects) in Fig. 4. One observes that the utilization of the NOP for model I results in 35% lower values for the electric field in comparison with those for both models II and III. However, the values for models II and III are very similar, suggesting we have reached an apparent convergence. It is important to emphasize that the slopes (i.e., the temperature dependence as given by the coefficient c_1) in Fig. 4 are almost identical, with only a small deviation for model I. This consistency leads to the conclusion that the procedure utilized in the present work to determine the temperature dependence of the electric field for liquid water is rather

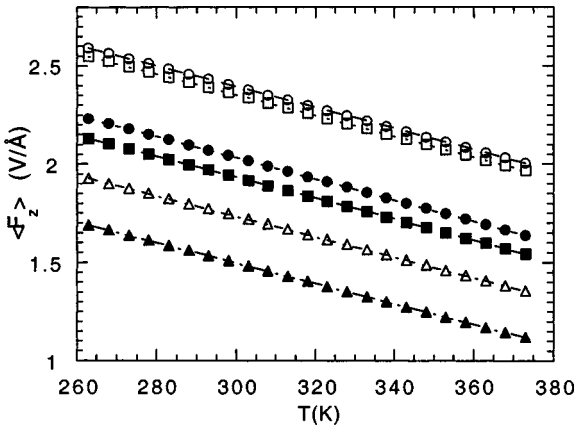

FIG. 4. Temperature dependence of the local electric field. The open triangles, squares, and circles represent models I, II, and III, respectively, utilizing TIP4P distribution characteristics. The corresponding solid symbols are results obtained with SPC/E distribution data.

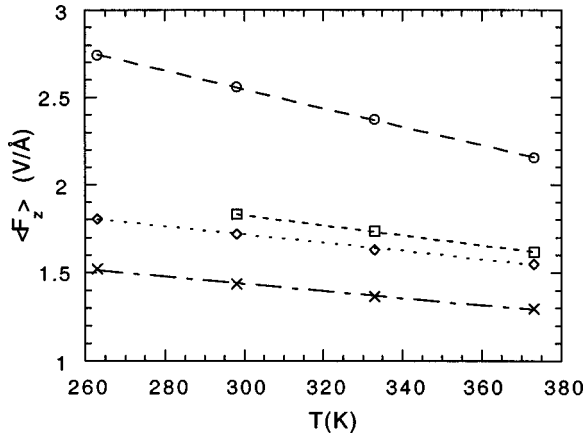

FIG. 5. Temperature dependence of the z component of the local electric field for the NEMO (Ref. 47) (circles), PPC (Ref. 15) (squares), SPC/E (triangles), and TIP4P (crosses) water models.

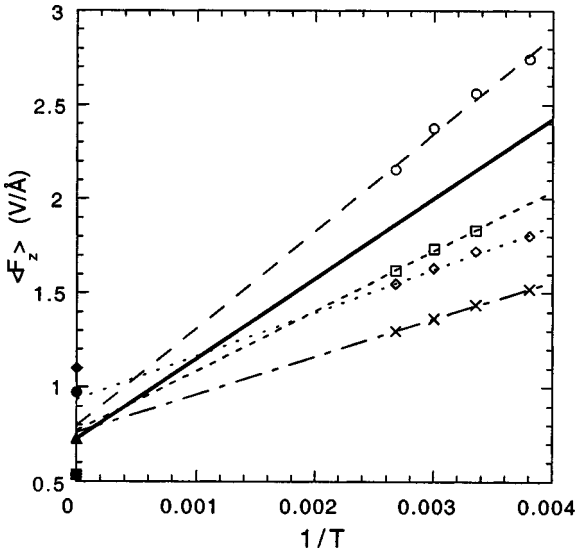

FIG. 6. Inverse-temperature dependence of the z component of the local electric field for the NEMO (Ref. 47) PPC (Ref. 15), SPC/E, and TIP4P water models (the open circles, squares, triangles, and crosses, respectively). The solid symbols represent c_0^* values for models II and III, and the solid line is the temperature dependence for model III_S.

robust. It is reassuring that this principal quantitative result does not depend strongly on the choice of liquid-phase model or characteristic parameters.

In Fig. 5 we report the temperature dependence of the z component of the local electric field experienced by a water molecule determined for the TIP4P,[44] SPC/E,[45] PPC,[15] and NEMO[47] potentials, where the latter two models are polarizable water potentials. We observe that in all four cases the fields obtained are very well represented as linear functions of temperature. Comparing Figs. 4 and 5, one can see that the slope of the results for the NEMO potential is close to the temperature dependence extracted here. The expectation that a fully polarizable potential, such as NEMO, will give a temperature dependence of the local electric field closest to that of ''real'' water, and that nonpolarizable potentials will underestimate the dependence, is entirely consistent with the present results. The actual magnitudes of the electric fields predicted, for example 2.04 and 2.55 V/Å for III_S and the NEMO potentials, respectively, at $T=298$ K, are in reasonable agreement.

For purposes of comparison two additional models based exclusively on NOP for an isolated (gas-phase) water molecule were examined, although not shown in Fig. 4. In one case, identified as model 0a, our theoretical analysis considered only the contributions of the hyperpolarizabilities β and γ to the effective molecular polarizability, $\overline{\alpha}^{\mathrm{eff}}$, and hence the predicted local field. In the second case, model 0b, the full set of nonlinear coefficients, including contributions from the high-order polarizability, B, has been utilized. For model 0a the value of electric field extracted at ambient temperature, 0.83 V/Å, appears rather low. Model 0b yields significantly larger values, 1.65 and 1.90 V/Å, when SPC/E or TIP4P distribution parameters, respectively, are employed. Clearly, the presence of the high-order (B) term is important in estimating the electrostatic environment within liquid water. The importance of the B (field gradient) term is not a consequence of its relatively large magnitude, but rather it is the result of the near cancellation of the two much larger contributions from β and γ. We again observe (see Table V) that the temperature dependence is very similar to that found with the other models.

C. Alternative analysis

There have been several instances in the above analysis [i.e., Eqs. (13), (14), (16), and (17)] where choices have been made with respect to specific functional forms. In making these choices we have always strived to use the simplest forms that still capture the essential behavior of the quantity of interest. We remark that in cases where we have attempted to employ higher-order forms, the results obtained have exhibited numerical instabilities (at least with the quality of the present data). In this section we will explore an alternate set of representations that allows us to examine the possible effects of the choices made.

It is clear from Fig. 3 that a quadratic fit of the effective molecular polarizability (derivative from refractive index data) to $1/T$ provides at least as good a representation of this data as our original quadratic in T. Thus in place of Eq. (16) we can write

$$\overline{\alpha}^{\mathrm{eff}} = b_0^* + b_1^*(1/T) + b_2^*(1/T)^2. \tag{25}$$

Moreover, if one presumes that the magnitude of the local field is indicative of the degree of local order in the liquid, then one might expect that in its simplest form

$$F_Z^0 = c_0^* + c_1^*(1/T). \tag{26}$$

In Fig. 6 we have replotted the data from Fig. 5 for the TIP4P, SPC/E, PPC, and NEMO water models against inverse temperature. We observe that, for the relatively narrow range of temperature spanned, the data again exhibit essentially linear behavior. If these lines are then extrapolated to infinite temperature, we discover that the values of the four y intercepts are almost coincident; the average of these four values is 0.82 V/Å. At infinite temperature we could expect the liquids to become structureless and hence for the average local field to approach zero. Clearly, there appears to be a systematic error arising in any linear extrapolation of normal

TABLE VI. Coefficients c_0^* and c_1^* for the inverse temperature treatment of the average local electric field as extracted from experimental refractive index data for liquid water.

Distribution coefficients	Model I		Model II		Model III	
	c_1^*	c_0^*	c_1^*	c_0^*	c_1^*	c_0^*
TIP4P	7.92	0.0075	8.12	0.0189	8.19	0.0214
SPC/E	7.97	0.0027	8.21	0.0104	8.26	0.0141

liquid-phase results to infinite temperature. Below, we will find that we can take advantage of this apparent constant correction.

An alternative treatment of refractive index data can now be developed by employing Eqs. (25) and (26) in place of Eqs. (16) and (17) in our formulation. This is an important verification since, if the results from the two routes are in agreement, we have strong support indicating that we have reasonably accounted for all critical physical behavior. Our development proceeds as before (see Sec. II) and we immediately obtain that

$$c_1^* = \sqrt{b_2^*/a_2}, \tag{27}$$

and

$$c_0^* = (b_1^*/c_1^* - a_1)/2a_2, \tag{28}$$

where the positive root is now appropriate in Eq. (27). Employing results from Table IV and Fig. 3(b), while taking into account the appropriate reference field conditions, we have obtained values for the coefficients c_0^* and c_1^*; these have been summarized in Table VI.

It is clear from Table VI that the temperature dependence (i.e., the value of the slope c_1^*) is very well reproduced within the various model treatments, whereas the absolute values (i.e., the constant terms c_0^*) again show more variation. Points representing c_0^* arising from model II and III treatments have been included in Fig. 6 along with the full temperature dependence for model III_S (the remaining three lines, which have been omitted for clarity, would have virtually identical slopes). We again observe a stronger temperature dependence for the average local field than is predicted by the nonpolarizable water potentials. Perhaps the most striking feature of Fig. 6 is that the values of c_0^* (for our two best models) appear clustered around the same common y intercept of the computer simulation results for waterlike liquids. Averaging these four values of c_0^*, we obtain 0.8 V/Å (in effectively exact agreement with the simulation average) with a standard deviation of ± 0.2 V/Å. The ability of this inverse-temperature treatment to provide this fix point can be viewed as an apparent advantage. It is this average of c_0^* and the corresponding average c_1^* that will be used below to determine our estimate for the total dipole moment for liquid water at ambient conditions.

D. The total dipole moment

The temperature dependence of the local electric field can now ultimately be used to obtain one of the most important physical parameters for the water molecule in condensed state, its (average) total molecular dipole moment, $\langle m \rangle$. The total dipole moment can be determined using results for the temperature dependence of the local electric field, $\langle F_z \rangle$, in the expression

$$\langle m \rangle = \mu_0 + \alpha_{zz} + \langle F_z \rangle, \tag{29}$$

where again μ_0 is the permanent (or gas-phase) dipole moment of the water molecule, and α_{zz} is the zz component of the polarizability obtained for the liquid-phase molecule.[10] We remark that for water one can expect the value of $\langle m \rangle$ to be close to that of $\langle |m| \rangle$. The temperature dependence of $\langle m \rangle$ has thus been obtained for the temperature range 263–373 K and explicit results for the total dipole moment are shown in Fig. 7.

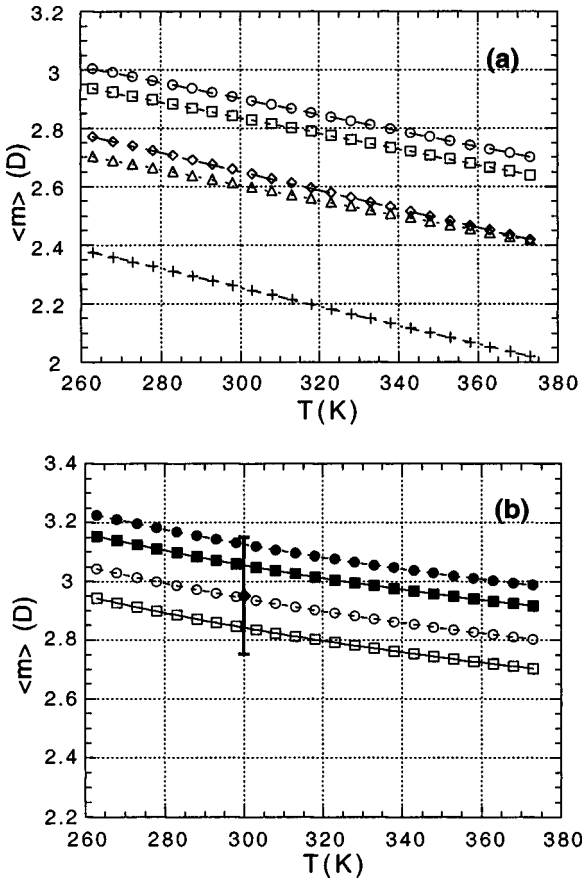

FIG. 7. Temperature dependence of the total dipole moment of liquid water. (a) Crosses, diamonds, triangles, squares, and circles represent values obtained from the linear-temperature treatment (see Sec. IV B) with models 0a, 0b, I, II, and III, respectively, together with SPC/E distribution characteristics. (b) Squares and circles represent values obtained from the inverse-temperature treatment (see Sec. IV C) with models II and III, respectively. Solid and open symbols correspond to use of TIP4P and SPC/E distribution parameters, respectively.

In Fig. 7(a) we present values obtained for all five mean-field models coupled with SPC/E distribution characteristics, where the average local fields are those determined assuming linear-temperature dependence (see Sec. IV B). In general, the numerical values for all models taken with the TIP4P parameters $d_{ii,1}$ and $e_{i,2}$ are somewhat larger over the entire temperature range, although they otherwise parallel the appropriate SPC/E curves [e.g., see Fig. 7(b)]. The temperature variation in $\langle m \rangle$ observed in Fig. 7(a) (linear-temperature treatment) for models I, II, and III combined with either TIP4P or SPC/E distribution data is consistently 9% (0.27 D) in going from 273 to 373 K. Almost identical behavior is evident in Fig. 7(b) (inverse-temperature treatment), where the decrease in the dipole moment is just slightly smaller (i.e., 0.21 D). This consistency clearly suggests that the present approach is able to predict accurately the temperature dependence in the average total molecular dipole moment for liquid water. The small difference in the temperature dependence determined from our two separate treatments provides confirmation that we have been successful in capturing the requisite physical behavior independent of the exact choice of our functional forms. The observed variation in the total dipole moment over this temperature range will be a sensitive measure of the change in local environment (or structure) experienced. The essentially linear behavior and an almost 10% decrease in $\langle m \rangle$ for a temperature increase from 273 to 373 K is in accord with several model studies for liquid water using fully polarizable potentials.[7,35]

Constancy in the absolute values of the average dipole moment obtained from the present extraction procedure for our various mean-field representations is less well reproduced, although there is a clear suggestion of convergence with the two most detailed models (II and III). As discussed in Sec. IV C, our treatment based on inverse temperature appears to afford our best estimate for the total molecular dipole moment for liquid water at ambient conditions; accordingly, a value of 2.95 ± 0.2 D is obtained. As discussed above in Sec. II, the neglect of short-range interactions in the present mean-field treatment is likely to have resulted in a slight overestimation of this value. The assigned error bar incorporates a ± 0.1 D contribution arising from the observed variation in c_0^*, which we believe reflects the major identifiable errors intrinsic to our approach. We have then simply doubled this value in an attempt to account for the total contribution of any remaining unidentified errors. This value for the average total dipole moment at ambient conditions is included in Fig. 7(b), and encompasses results for all models II and III from either linear- or inverse-temperature treatments. In Fig. 7(a) the numerical values of the total dipole moment at 300 K for model I (2.6 D), for model 0b (2.65 D), and especially for model 0a (2.3 D) are apparently underestimated, and are comparable with lower estimates available in the literature (see Table I), including the magnitudes reported by Delle Site *et al.*[2] The dipole moment obtained in the present work at 300 K corresponds extremely well with results reported by Batista *et al.*[5] and by Silvestrelli and Parrinello.[8] Moreover, it is in excellent agreement with that of Badyal *et al.*,[9] the only experimentally determined value currently available in the literature. It is important to point out that previous investigations[2,10] have indicated that there is also a significant increase in the quadrupole moment (10%–15%) of a liquid-phase water molecule relative to gas phase. It is obviously crucial for a water model to reproduce both the elevated dipole and quadrupole moments of the molecule in order to recover, for example, the correct dielectric properties of the real liquid.[33,35]

As discussed in the Introduction, several different comparisons with estimates from the literature for the average total dipole moment are possible; yet, not only is there considerable spread in these literature estimates, but many are based upon ice models. It could be expected that the value for $\langle m \rangle$ for liquid water in its supercooled state should be close to, and somewhat less than, that for ice. At 263 K we would estimate the total dipole moment to lie within a range from 2.8 to 3.2 D. This can be reasonably compared with estimates reported in the literature for ice. For example, it is in excellent agreement with that reported by Batista *et al.*[3] for ice I_h. Reis *et al.*[26] have presented numerical results for different ice polymorphs using a discrete local-field approximation. Their values range from 2.53 D for ice I_h to 2.86 D for ice II, but could be considered to be slight underestimates because the polarization effect of the field gradient has not been taken into account in their theoretical framework. Interestingly, the estimates for the average high-order molecular electronic properties determined within the permanent electric dipole crystal fields of Ref. 26 are also in good agreement with the hyperpolarizabilities utilized in the present investigation.

V. CONCLUSIONS

In this article we have reported a means by which the average total dipole moment for the water molecule can be extracted from very reliable experimental (refractive index together with density) data. To accomplish this, three critical components are required: a general formalism that relates an effective molecular polarizability to the average local electric field experienced by the water molecule in the liquid state, a qualitative description of the distributions of the local electric field and field gradient, and accurate results for the molecular response properties of a liquid-phase water molecule. Results for the first two components have been presented here, together with the resultant values for average local electric fields and total molecular dipole moments over the normal temperature range for liquid water.

Within the general formalism developed in this work, the perturbing local environment affecting a liquid water molecule is represented with a local electric field. The influence of the local environment upon the electric response properties of the molecule is considered within the context of classical electrostatics. The change in the effective polarizability of the molecule, which can be extracted from refractive index data and characterizes nonlinear behavior, is used to quantify the local electric field and its temperature dependence.

In order to perform our analysis, basic characteristics of the distributions of electric fields and field gradients experienced by a water molecule in the liquid are required. The necessary parameters (distribution widths and proportionality

constants) were obtained from MD simulations employing the SPC/E[45] and TIP4P[44] water models for liquid systems from 263 to 373 K. These models were chosen since they are standard potentials that describe well the local structure in liquid water. The values finally obtained for the local electric field and total dipole moment demonstrate some sensitivity to the distribution parameters and therefore to the choice of potential model; however, their relative temperature dependence is extremely well reproduced. This suggests that from the insights gained in this study a better choice of potential model for characterizing the field distributions should be possible.

The choice of reference conditions about which the molecular response properties were expanded was also recognized as important (also see Ref. 10). The contributions of field gradient terms were found to be significant due to near-cancellation of the larger contributions from first- and second hyperpolarizabilities. Again, the insights gained from this work provide a basis on which to make a better selection of the liquid-state reference conditions. Improvements in the characterization of the required properties of the field and field gradient distributions, together with a superior choice of the reference conditions, should allow for further refinements of the results reported here.

The total molecular dipole moment for liquid water as extracted in this study from the temperature dependence of experimental refractive index data exhibits an almost 10% decrease in going from 273 to 373 K. The consistent behavior observed in our results gives us considerable confidence in our ability to quantify this trend. The present approach also provides estimates for the absolute values for the total dipole moment. At ambient conditions our analysis yields a dipole moment of 2.95 ± 0.2 D, in excellent agreement with other studies. The present results should be useful both in characterizing the local environment in liquid water and in confirming the reliability of theoretical models.

ACKNOWLEDGMENT

The aughors are grateful for the financial support of the Natural Science and Engineering Research Council of Canada.

APPENDIX: EXPRESSIONS FOR $\Delta\alpha_{ii}$ AND a_i

Taking advantage of symmetry conditions for the water molecule and retaining only nonzero terms, explicit expressions for the diagonal components of the change in the effective molecular polarizability become

$$\Delta\alpha_{xx}(\underline{F},\nabla\underline{F}) = \beta_{xxz}F_z + 1/2\,\gamma_{xxzz}F_z^2 + 1/2\,\gamma_{xxxx}F_x^2 + 1/2\,\gamma_{xxyy}F_y^2 + 1/3B_{xxxx}\nabla F_{xx} + 1/3B_{xxyy}\nabla F_{yy} + 1/3B_{xxzz}\nabla F_{zz}, \quad \text{(A1a)}$$

$$\Delta\alpha_{yy}(\underline{F},\nabla\underline{F}) = \beta_{yyz}F_z + 1/2\,\gamma_{yyzz}F_z^2 + 1/2\,\gamma_{yyyy}F_y^2 + 1/2\,\gamma_{yyxx}F_x^2 + 1/3B_{yyyy}\nabla F_{yy} + 1/3B_{yyxx}\nabla F_{xx} + 1/3B_{yyzz}\nabla F_{zz}, \quad \text{(A1b)}$$

and

$$\Delta\alpha_{zz}(\underline{F},\nabla\underline{F}) = \beta_{zzz}F_z + 1/2\,\gamma_{zzzz}F_z^2 + 1/2\,\gamma_{zzxx}F_x^2 + 1/2\,\gamma_{zzyy}F_y^2 + 1/3B_{zzzz}\nabla F_{zz} + 1/3B_{zzxx}\nabla F_{xx} + 1/3B_{zzyy}\nabla F_{yy}. \quad \text{(A1c)}$$

Using Eq. (10) together with Eqs. (11)–(14), it can be shown that the coefficients in Eq. (15) are given by

$$a_1 = 1/3(\beta_{xxz} + \beta_{yyz} + \beta_{zzz}) + 1/9d_{xx,1}(B_{xxxx} + B_{yyxx} + B_{zzxx}) + 1/9d_{yy,1}(B_{xxyy} + B_{yyyy} + B_{zzyy}) + 1/9d_{zz,1}(B_{xxzz} + B_{yyzz} + B_{zzzz}), \quad \text{(A2a)}$$

and

$$a_2 = 1/6(1 + e_{z,2})(\gamma_{xxzz} + \gamma_{yyzz} + \gamma_{zzzz}) + 1/6e_{x,2}(\gamma_{yyxx} + \gamma_{zzxx} + \gamma_{xxxx}) + 1/6e_{y,2}(\gamma_{xxyy} + \gamma_{zzyy} + \gamma_{yyyy}). \quad \text{(A2b)}$$

[1] C. A. Coulson and D. Eisenberg, Proc. R. Soc. London, Ser. A **291**, 445 (1966).
[2] L. Delle Site, A. Alavi, and R. M. Lynden-Bell, Mol. Phys. **96**, 1683 (1999).
[3] E. R. Batista, S. S. Xantheas, and H. Jonsson, J. Chem. Phys. **109**, 4546 (1998).
[4] D. Adams, Nature (London) **293**, 447 (1981).
[5] E. R. Batista, S. S. Xantheas, and H. Jonsson, J. Chem. Phys. **111**, 6011 (1999).
[6] E. R. Batista, S. S. Xantheas, and H. Jonsson, J. Chem. Phys. **112**, 3285 (2000).
[7] S. W. Rick, J. Chem. Phys. **114**, 2276 (2001).
[8] P. L. Silvestrelli and M. Parrinello, Phys. Rev. Lett. **82**, 3308 (1999).
[9] Y. S. Badyal, M.-L. Saboungi, D. L. Price, S. D. Shastri, D. R. Haeffner, and A. K. Soper, J. Chem. Phys. **112**, 9206 (2000).
[10] A. V. Gubskaya and P. G. Kusalik, Mol. Phys. **99**, 1107 (2001).
[11] Y. Tu and A. Laaksonen, Chem. Phys. Lett. **329**, 283 (2000).
[12] J. K. Gregory, D. C. Clary, K. Liu, M. G. Brown, and R. J. Saykally, Science **275**, 814 (1997).
[13] K. Laasonen, M. Sprik, M. Parrinello, and R. Car, J. Chem. Phys. **99**, 9080 (1993).
[14] B. D. Bursulaya, J. Jeon, D. A. Zichi, and H. J. Kim, J. Chem. Phys. **108**, 3286 (1998).
[15] I. M. Svischev, P. G. Kusalik, J. Wang, and R. J. Boyd, J. Chem. Phys. **105**, 4742 (1996).
[16] D. N. Bernardo, Y. Ding, K. Krogh-Jespersen, and R. M. Levy, J. Phys. Chem. **98**, 4180 (1994).
[17] A. A. Chialvo and P. T. Cummings, J. Chem. Phys. **105**, 8274 (1996).
[18] A. Wallqvist and R. D. Mountain, in *Reviews in Computational Chemistry*, edited by K. B. Lipkowitz and D. B. Boyd (Wiley, New York, 1999), Vol. 13, pp. 183–247.
[19] M. Sprik and M. L. Klein, J. Chem. Phys. **89**, 7556 (1988).
[20] K. Liu, M. G. Brown, and R. J. Saykally, J. Phys. Chem. A **101**, 8995 (1997).
[21] L. X. Dang and T.-M. Chang, J. Chem. Phys. **106**, 8149 (1997).
[22] D. Wei and D. R. Salahub, Chem. Phys. Lett. **224**, 291 (1994).
[23] E. S. Fois, M. Sprik, and M. Parrinello, Chem. Phys. Lett. **223**, 411 (1994).
[24] C. Gatti, B. Silvi, and F. Colonna, Chem. Phys. Lett. **247**, 135 (1995).
[25] M. I. Heggie, C. D. Latham, S. C. P. Maynard, and R. Jones, Chem. Phys. Lett. **249**, 485 (1996).
[26] H. Reis, S. G. Raptis, and M. G. Papadopoulos, Chem. Phys. **263**, 301 (2001).
[27] M. Sprik, J. Chem. Phys. **95**, 6762 (1991).
[28] P. W. Fowler and P. A. Madden, Phys. Rev. **30**, 6131 (1984).
[29] P. W. Fowler, F. Ding, and R. W. Munn, Mol. Phys. **84**, 787 (1995).
[30] P. Jemmer, P. W. Fowler, M. Wilson, and P. A. Madden, J. Phys. Chem. **102**, 8377 (1998).
[31] P. Jemmer, M. Wilson, P. A. Madden, and P. W. Fowler, J. Chem. Phys. **111**, 2038 (1999).
[32] P. W. Fowler, H. M. Kelly, and N. Vaidehi, Mol. Phys. **82**, 211 (1994).

[33] S. L. Carnio and G. N. Patey, Mol. Phys. **47**, 1129 (1982).
[34] J. M. Caillol, D. Levesque, J. J. Weis, P. G. Kusalik, and G. N. Patey, Mol. Phys. **55**, 65 (1985).
[35] P. G. Kusalik and G. N. Patey, Mol. Phys. **65**, 1105 (1988).
[36] P. G. Kusalik and G. N. Patey, J. Chem. Phys. **92**, 1345 (1990).
[37] A. J. Stone, *The Theory of Intermolecular Forces* (Clarendon, Oxford, 1996).
[38] J. A. Lorentz, Ann. Phys. (Leipzig) **9**, 641 (1880); L. Lorentz, *ibid.* **11**, 70 (1880).
[39] I. Thormahlen, J. Straub, and U. Grigull, J. Phys. Chem. Ref. Data **14**, 933 (1985).
[40] P. Schiebener, J. Straub, J. M. H. Levelt Sengers, and J. S. Gallagher, J. Phys. Chem. Ref. Data **19**, 677 (1990).
[41] G. Stell, G. N. Patey, and J. S. Hoye, Adv. Chem. Phys. **48**, 185 (1981).
[42] J. S. Hoye and G. Stell, J. Chem. Phys. **75**, 3565 (1981).
[43] While it is necessary to restrict the analysis in our formulation to changes in the molecular polarizability, there could be significant improvement in the quality of the results if it were possible to utilize absolute values.
[44] W. L. Jorgensen, J. Chandrasekhar, J. D. Madura, R. W. Impley, and M. L. Klein, J. Chem. Phys. **79**, 926 (1983).
[45] H. G. C. Berendsen, J. R. Grigera, and T. P. Straatsma, J. Phys. Chem. **91**, 6269 (1987).
[46] M. P. Allen and D. J. Tildesley, *Computer Simulation of Liquids* (Clarendon, Oxford, 1987), pp. 156–162.
[47] T. M. Nymand and P.-O. Astrand, J. Chem. Phys. **106**, 8332 (1997).
[48] T. M. Nymand, P.-O. Astrand, and K. V. Mikkelsen, J. Phys. Chem. B **101**, 4105 (1997).
[49] A. Wallqvist and G. Karlstrom, Chem. Scr. **29A**, 131 (1989).
[50] P.-O. Astrand, P. Linse, and G. Karlstrom, Chem. Phys. **191**, 195 (1995).
[51] L. W. Tilton and J. K. Taylor, J. Res. Natl. Bur. Stand. **20**, 419 (1938).
[52] Ch. Saubade, J. Phys. (France) **42**, 359 (1981).
[53] E. E. Hall and A. R. Payne, Phys. Rev. **20**, 249 (1922).